Alzheimer's Patient Analysis Using Image and Gene Expression Data and Explainable-AI to Present Associated Genes

Md. Sarwar Kamal, Aden Northcote, Linkon Chowdhury, Nilanjan Dey, *Senior Member, IEEE*, Rubén González Crespo, *Senior Member, IEEE*, and Enrique Herrera-Viedma, *Fellow, IEEE*

***Abstract*— There are more than 10 million new cases of Alzheimer's patients worldwide each year, which means there is a new case every 3.2 s. Alzheimer's disease (AD) is a progressive neurodegenerative disease and various machine learning (ML) and image processing methods have been used to detect it. In this study, we used ML methods to classify AD using image and gene expression data. First, SpinalNet and convolutional neural network (CNN) were used to classify AD from MRI images. Then we used microarray gene expression data to classify the diseases using k-nearest neighbors (KNN), support vector classifier (SVC), and Xboost classifiers. Previous approaches used only either images or gene expression, while we used both data together and also explained the results using trustworthy methods. it was difficult to understand how the classifiers predicted the diseases and genes. It would be useful if the results of these classifiers could be explained in a trustworthy way. To establish trustworthy predictive modeling, we introduced an explainable artificial intelligence (XAI) method. The XAI approach we used here is local interpretable model-agnostic explanations (LIME) for a simple human interpretation. LIME interprets how genes were predicted and which genes are particularly responsible for an AD patient. The accuracy of CNN is 97.6%, which is 10.96% higher than the SpinlNet approach. When analyzing gene expression data, SVC provides higher accuracy than other approaches. LIME shows how genes were selected for a particular AD patient and the most important genes for that patient were determined from the gene expression data.**

***Index Terms*— Convolutional neural network (CNN), gene expression measurements, k-nearest neighbors (KNN), local interpretable model-agnostic explanations (LIMEs), SpinalNet, support vector classifier (SVC), Xboost.**

Manuscript received May 27, 2021; revised August 6, 2021; accepted August 11, 2021. Date of publication August 24, 2021; date of current version September 10, 2021. The Associate Editor coordinating the review process was Alice Buffi. *(Corresponding author: Rubén González Crespo.)*

Md. Sarwar Kamal and Aden Northcote are with the School of Computer Science, Faculty of Engineering and IT, University of Technology Sydney, Ultimo, NSW 2007, Australia (e-mail: mdsarwar.kamal@uts.edu.au; aden.j.northcote@student.uts.edu.au).

Linkon Chowdhury is with the Computer Science and Engineering, East Delta University, Chattogram 4209, Bangladesh (e-mail: linkon.c@eastdelta.edu.bd).

Nilanjan Dey is with the Department of Computer Science and Engineering, JIS University, Kolkata 700109, India (e-mail: nilanjan.dey@jisuniversity.ac.in).

Rubén González Crespo is with the Department of Computer Science and Artificial Intelligence, Universidad Internacional de La Rioja, 26006 Logroño, Spain (e-mail: ruben.gonzalez@unir.net).

Enrique Herrera-Viedma is with the Department of Computer Science and Artificial Intelligence, University of Granada, 18071 Granada, Spain (e-mail: viedma@decsai.ugr.es).

Digital Object Identifier 10.1109/TIM.2021.3107056

I. Introduction

ALZHEIMER disease (AD) is a progressive and degenerative disease of the brain that is the most common cause of dementia worldwide [1]–[3]. In 2020, there were 50 million Alzheimer's patients and by 2050, there will be approximately 150 million Alzheimer's patients. AD places an extreme burden on patients, caregivers, and healthcare systems, with research suggesting that the number of AD patients is likely to increase dramatically in the coming decades without the development of preventive treatments with modern medical tools [4]–[7]. Despite the prevalence and severity of the disease, currently available diagnostic tests cannot provide definitive results within a patient's lifetime and often rely on a detailed understanding of the patient's medical history and medical information [1]. Histologic examination of affected brain tissue samples provides the most accurate AD diagnosis, but the collection of these samples via biopsy is contraindicated for AD due to the high risk to the patient [8]. Research also suggests that brain changes due to AD may begin decades before the onset of clinical symptoms of AD [9], leading to the introduction of a preclinical stage of dementia called mild cognitive impairment (MCI) [10]. The benefit of diagnosis for patients at this preclinical stage of the disease is substantial [11]. However, not all patients who receive a diagnosis of MCI develop AD. Diagnostic tests capable of reliably detecting AD at any stage of the disease would be of great value to both patients and future research.

Accelerated by the availability of open ADrelevant databases, great strides have been made in the application of machine learning (ML) techniques to the diagnosis of AD, particularly through magnetic resonance imaging (MRI). The presence of neurological changes induced by AD MRI is well established [12]–[14], as is the effectiveness of ML techniques that use these data to make inaccurate diagnostic decisions [15] measurement. In contrast, the relevance of genetic markers in the development of AD has long been known [16]–[20], but the use of these data in ML-based diagnostic models has been rather limited. Moreover, a significant correlation has been found between gene expression data and AD [21], [22], with recent research showing promising use of these data in diagnosis [23], contributing to better treatment with medical tools. Many ML-based approaches to AD diagnosis over this data

1557-9662 © 2021 IEEE. Personal use is permitted, but republication/redistribution requires IEEE permission.
See https://www.ieee.org/publications/rights/index.html for more information.

Authorized licensed use limited to: VIT University- Chennai Campus. Downloaded on November 08,2022 at 05:47:25 UTC from IEEE Xplore. Restrictions apply.

are based on traditional ML algorithms such as support vector machines and rely on prior feature extraction. While many such feature extraction methods exist, deep learning (DL) via multilayer artificial neural networks (ANNs) known as deep neural networks (DNNs) offers a promising alternative by enabling automatic feature extraction. While DL approaches have historically been disadvantaged by their "black-box" classification decisions, recent advances in "explainable" DL models have begun to mitigate this disadvantage [24].

In practice, the implementation of DNNs requires the consideration of a large number of inputs and parameters, which leads to a high computational cost. Much of the previous research has relied on prior feature extraction to reduce the dimensionality of real-world inputs such as MRI and gene expression data [15]. While this approach can lead to high accuracy, it can also lead to models failing to account for new correlations that exist in the raw data [25], [26]. New approaches to the architecture of DNNs, such as spiral neural networks (SNNs) and convolutional neural networks (CNNs), allow the dimensionality of the input data to be reduced as part of the model's learning process, allowing the model to work directly with the raw input [27], [28]. By applying these DNN architectures to gene expression data and MRI in tandem, we hope to identify features and correlations useful for predicting AD diagnosis.

The value of MRI in AD diagnosis is well established and has been included in several proposed new AD diagnostic criteria [29], [30]. High-resolution MRI is able to detect the presence and degree of brain atrophy, which can support *in vivo* diagnosis AD [31] and even indicate the presence of neurofibrillary tangles (NFTs), which are considered a hallmark pathology of AD [32]. While brain atrophy measured by MRI is a reliable and sensitive measure of neurodegeneration in general [13], it is a measure that lacks specificity for AD, as many other forms of dementia can result in similar patterns of atrophy [31]. Moreover, an absence of measurable atrophy does not preclude an AD diagnosis [14]. For these reasons, a reliable diagnosis of AD cannot be made on the basis of MRI alone.

Correlations between gene expression data and AD have been found, with recent research showing promise for use in ML-based approaches to AD diagnosis [23]. Independent of AD diagnosis [22], a high degree of individual variation was found in gene expression data, forcing restrictive trait selection methods when searching for AD relevant expression data.

By combining MRI and gene expression data, we can implement multimodal diagnostic models and provide a more comprehensive dataset for AD diagnosis that mitigates the lack of specificity inherent to the exclusive use of the two data types. Here we investigate the function and effectiveness of two different DNN architectures, the Spinal Neural Network and the CNN. To address the "black box" problem of many DNN implementations, we outline the implementation of locally interpretable model-agnostic explanations (LIME) that allow for easy human interpretation of the results. MRI and gene expression data are preprocessed and used to train these models and evaluate their performance via standard

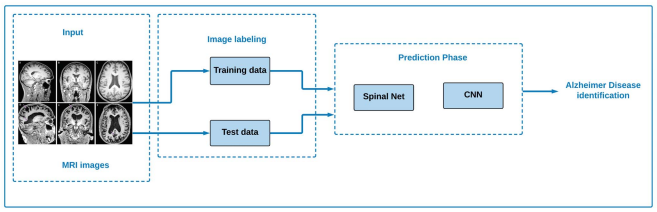

Fig. 1. Proposed method for AD analysis from MRI images.

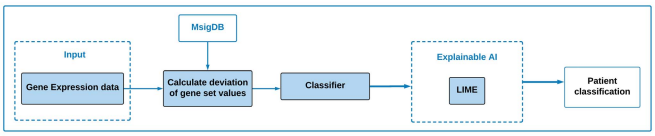

Fig. 2. Proposed method for AD from gene expression.

ML metrics such as accuracy, precision, recall, and f-measure measurement.

This article is organized as follows. Section II is the method whether we described SpinalNet, CNN, different classifiers for prediction and locally interpretable method, LIME for explaining significant genes. Section III results from whether we describe the simulation results and comparison, and Section IV concludes this article.

II. Methodology

After careful consideration, it was decided that this method best met the requirements for AD MRI image analysis and gene expression data processing. Two paths were followed. In the first path, MRI images were examined using SpinalNet and CNN. The second path involves classifiers and explainable AI (XAI) to identify genes associated with AD for a given patient. SpinalNet and CNN were applied to four AD classes: mild dementia, moderate dementia, non-dementia, and very mild dementia. MRI images were divided into test and training data in these four classes, and the prediction framework described in Fig. 1.

In gene expression analysis, we used gene microarray data to predict AD with different classifiers. We used support vector classifiers (SVC), k-nearest neighbors (KNN), and Xboost. We also found significant genes for AD using the method of explainable AI, i.e., local interpretable model-agnostic explanations (LIME) that interpret how the classifier predicted the disease with respect to specific genes (Fig. 2).

A. SpinalNet for Alzheimer Prediction

The human brain receives a lot of information from various organs that sense pressure, heat, vibration, state of things, etc. The human spinal cord is the backbone of the nervous systems that receive sensory input from various parts of the body. The SpinalNet works on the basis of the spinal cord and the human brain and is similar to the architecture of neural networks. However, the SpinalNet is slightly different from a DNN with fewer computations, fewer connections, and layers. This article describes the basic SpinalNet model and framework for AD in Fig. 3.

Authorized licensed use limited to: VIT University- Chennai Campus. Downloaded on November 08,2022 at 05:47:25 UTC from IEEE Xplore. Restrictions apply.

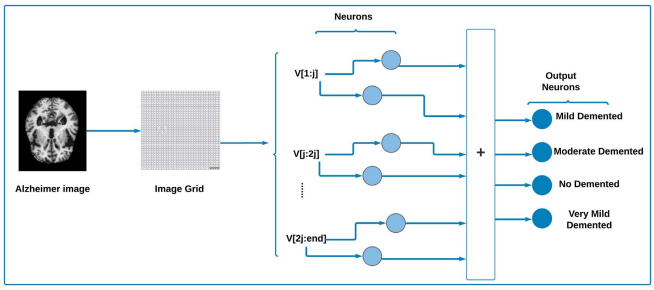

Fig. 3. Framework of SpinalNet for AD.

1) Architecture of the Network: This model consists of frequency-encoding time-dependent neurons with weight and membrane potential. We used pixel values from MRI images for each neuron. Let w_{ij} be the weight of neurons from j to i, a_j be the activity parameter of the jth neuron, and the property time of a neuron be τ.

The potential membrane of the i-th neuron is V_i, which can be derived from the following differential equation:

$$\tau \frac{dV_i}{dt} = -V_i + \sum_j w_{ij} a_j. \tag{1}$$

Each image intensity is considered as a membrane potential — the sum of all projections from neuron j to neuron i. The output of the activity parameter a_j is a nonlinear function of the membrane potential, which is as follows.

$$a_j = \phi(V_i). \tag{2}$$

This function is expressed by a sigmoid function with slope parameter α in the following equation:

$$\phi(V_i) = \frac{1}{(1 + \exp(-\alpha V_i))}. \tag{3}$$

This sigmoid function is applied in the jth to ith neuron to filter the image intensity. The standard sigmoid function uses the membrane potential V_i with values between 0 and 0.5. The shift problem of this sigmoid function should be the normalized function as follows:

$$\phi(V_i) = \frac{2 - 2\gamma}{1 + (-\alpha V_i)} - 1 + 2\gamma, \quad \text{for } V_i \geq 0. \tag{4}$$

This equation identified those pixels that value more than 1, which indicates the white region. For $V_i < 0$ an exponential function has been shown as

$$\phi(V_i) = \gamma \exp\left(\frac{1 - \gamma}{2\gamma} \alpha V_i\right), \quad \text{for } V_i < 0. \tag{5}$$

The weights w_{ij} are updated according to Hebb's rule, which has been modified for reducing unbounded growth of neurons inputs. Updated normalized weight is

$$\Delta w_{ij} = \eta a_i (a_j - a_i w_{ij}). \tag{6}$$

Here, η is the learning parameter and Δw_{ij} is the updated weights. Weight is updated until to find the target class of AD. The SpinalNet contains several different types of motor neurons with the following activity function:

$$a_i = \frac{1}{(1 - \theta_i)^2} \phi(V_i). \tag{7}$$

Each pixel value triggers motor neurons with their activity function. These motor neurons connect with each other to form clusters. When the neurons become active, the clusters perform a spontaneous activity called space for the wire (SAC). SAC generates a signal while the input neurons receive pixel values and train the model. Training and testing the network approach are described in the next section.

2) Training the Network: The signal generator of SAC generates a sinusoidal signal using the following equation while obtaining values from the image

$$f(t) = \sin(\omega t + \delta). \tag{8}$$

In the training phase, each period of the signal generator is divided into 100 bins, and in each bin the network is updated. First, the baseline values for the corresponding signal bin were calculated from the activities of the motor neuron clusters in the SACs. Then, the other activities of the neurons in the SACs clusters were calculated. The neurons in the first layer were updated using (1), (3), and (4).

In the second layer, the neurons in the clusters of motor neurons were updated using (1), (3), (4), and (7). Then, all the weights are updated using (6).

3) Testing the Network: After the network stabilizes in the training phase, we test the network for our Alzheimer dataset on test classes. During the testing phase, the motor neurons generate the signal for each SACs cluster for four test classes. Each test class has different constant signals. For example, the signal of the "Mild Dementia" class is identical to the signal of the "Moderate Dementia" class. So the motor neurons generate a separate signal for each class. Then the signal of the test class is matched with the signal of the training class. If the potential of the training class signal matches the potential of the test class signal, then we have found the class for the corresponding signal from the training clusters.

B. Convolutional Neural Network Alzheimer Disease

In addition to SpinalNet, we also used CNN to classify AD using MRI images. CNN is a special DL method for image processing problems, especially for image classification and object recognition, etc.

CNN consists of multiple convolutional layers, pooling layers, and dense layers. In CNN, the convolutional layers and pooling layers perform feature extraction of AD (affected regions) to distinguish the features between the affected regions [33]. We mapped the features using multiple kernels because we only select one feature whether the regions are affected by AD or not. The rectified linear unit (ReLU) activation function was used to calculate the values.

Then, polling layers reduce the area from MRI that is not associated with Alzheimer's affected region. Moreover, polling layers also reduce the computational cost. We applied Max Polling in the query layers to increase the computational efficiency. We have used a number of convolutional layers and pooling layers that identify the features. The last pooling layer is connected with the dense layer with the flat layer which is fully connected. The learning process takes place in the dense layer and classifies our images. When images are misclassified,

Authorized licensed use limited to: VIT University- Chennai Campus. Downloaded on November 08,2022 at 05:47:25 UTC from IEEE Xplore. Restrictions apply.

we adjust the weights of the neurons in the dense layer to increase the accuracy.

C. Classification of Gene Expression Data

In addition to classifying AD using MRI images, we have also applied classifiers using gene expression data. Here, we applied three different classifiers to predict the AD class. The first and most descriptive classification algorithm is KNN, a basic data classification method. KNN determines the class level for test samples based on the Euclidean distance of the samples to the training samples [34]. From the Alzheimer's microarray data, KNN classifies whether it is Alzheimer's or not based on the Euclidean distance. Another classifier is an ensemble method, namely Xboost. Xboost is a decision tree based ensemble method of ML. This method works based on a gradient boosting framework to strengthen weak learners [35]. Xboost also predicts AD. Finally, we applied SVC, one of the most popular predictive solution optimization techniques. It provides an optimal solution, and discriminative techniques have increased its acceptance for data mining and data classification [36]. We get better accuracy when we use SVC for our prediction.

D. Explainable AI for Predictive Model

Understanding how to correctly predict outcomes and explain a predictive model is extremely important. Currently, explainable AI (XAI) is becoming increasingly popular due to its ease of understanding and interpretable mechanisms. LIME [37] is a popular XAI method for interpreting predictive models. We applied LIME to explain our prediction results. LIME is a novel technique that explains the prediction process of any classifier by a locally interpretable process. LIME explains the classifier's prediction process and describe the correlation between genes that affect the AD prediction process. Here we describe the process the interpretable process of LIME. LIME uses a representation to quickly understand which key features are used in the prediction model. LIME uses the following methods, which use a faithful and interpretable explainer. Let X be the feature space and x be the feature instance of the Alzheimer data points. We explain our prediction model using LIME. In LIME, there are two important components, namely the explainer (f) and the black-box model (p). LIME uses an interpretable function to explain the process locally

$$\exp(x) = \text{argmin}_{f \epsilon F} \theta(p, f, \lambda_x) + \Omega(f). \tag{9}$$

Here $\exp(x)$ is the interpretable feature explained by LIME, $\theta(p, f, \lambda_x)$ is the loss function, p is the black-box model (i.e. SVC), f is the explainer, λ_x is the similarity measure between data points x, and Ω is the penalty for the complexity model f. Solve the equation 9 using anomaly data, and LIME explains the responsible Alzheimer's genes based on the classifier.

III. Experimental Result

The results are presented here both visually and numerically. Using these data, the results section is divided into several subsections; first, the collected data are described, and the next subsection deals with data pre-processing. A comparative analysis for image results and classifiers is described in the following subsections, and the last section describes the results of XAI.

TABLE I
DESCRIPTION OF THE MRI IMAGES FOR EACH CLASS

Methods	Sample size of Alzheimer disease classes			
	Mild Demented	Moderate Demented	Non Demented	Very Mild Demented
Training	717	52	2560	1792
Test	179	12	640	448

A. Data Description

In this study, we evaluate our proposal using MRI images of AD and microarray gene expression. We collected MRI images from Kaggle (www.kaggle.com/tourist55/alzheimers-dataset-4-class-of-images) with four different AD classes (mild dementia, moderate dementia, no dementia, and very mild dementia). Of the 6400 MRI images collected, 5121 are training images and the rest are used as test images. The total number of test and training images in each class is described in Table I. We used additional MRI images from the dataset OASIS -3 to validate our prediction (https://central.xnat.org) [38], [39]. We also collected gene expression data from the NCBI database (accession number GSE174367), which contains 104 gene expression data from patients. In these gene expression data, the rows contain the 18 234 genes and the columns contain the patients who have either AD or non-AD [40].

B. Data Pre-Processing

In the pre-processing phase, we process the grayscale MRI images into black and white images using the binarization procedure [41]. We used Otsu's binarization technique for grayscale image convertion. Black and white images have fewer pixel values than grayscale images, which reduces the computational cost. The preprocessed images are shown in Fig. 4 for the four classes. These binary images reduce the unnecessary areas related to AD, and the white areas are the essential part of our experiment.

C. Comparative Analysis of SpinalNet and CNN

The results of the two experiments with SpinalNet and CNN are presented here. SpinalNet first trained the model for the given classes and then predicts the test class for corresponding test images. Fig. 5 shows a partial scenario of training images for four classes for SpinalNet operation. We used 5121 images for training the network, and for each class, the network generates a unique signal. Based on the measurement of the signals, SpinalNet predicts the class for test images. We removed noise from our test and training MRI images using Gaussian filtering [42]. After removing the noise, the accuracy of the CNN and SpinalNet methods improves significantly.

We also performed AD class prediction using CNN. The evaluation metrics we considered include accuracy (10), precision (11), recall (12) and F-measure (13) for

Authorized licensed use limited to: VIT University- Chennai Campus. Downloaded on November 08,2022 at 05:47:25 UTC from IEEE Xplore. Restrictions apply.

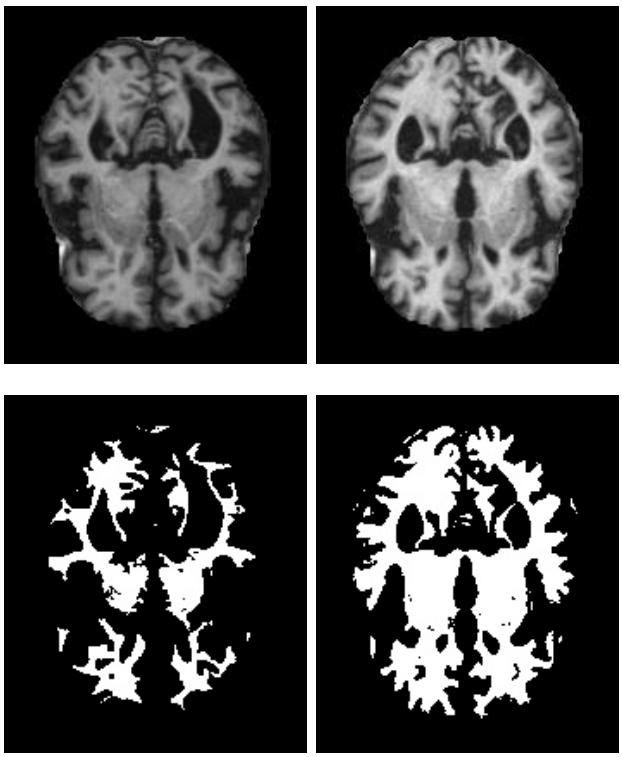

Fig. 4. Gray images for mild Dementia and moderate Dementia AD and conversion of these images to binary images.

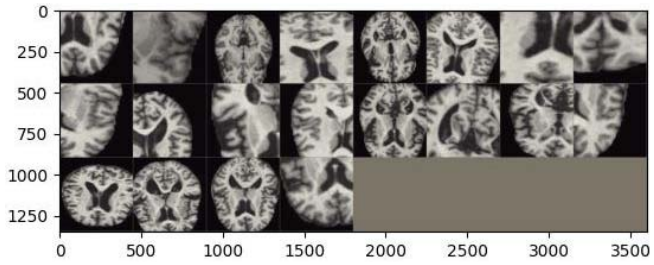

Fig. 5. Training images for SpinalNet.

the comparative studies

$$\text{Accuracy} = \frac{\text{TP} + \text{TN}}{\text{TP} + \text{TN} + \text{FP} + \text{FN}} \tag{10}$$

$$\text{Precision} = \frac{\text{TP}}{\text{TP} + \text{FP}} \tag{11}$$

$$\text{Recall} = \frac{\text{TP}}{\text{TP} + \text{FN}} \tag{12}$$

$$\text{F-measure} = 2 * \frac{\text{Precision} * \text{Recall}}{\text{Precision} + \text{Recall}}. \tag{13}$$

Table II shows the accuracy rate for four different classes. CNN provides the highest accuracy for all classes. The accuracy for moderate dementia with CNN is 97.2%, while the accuracy of SpinalNet is 87.3%. The accuracy of CNN for mild dementia and very mild dementia is 96.6% and 98.1%, respectively. The results of SpinalNet are less accurate due to the number of different signals from the training data. In some cases, the signals from the test images did not properly match the training signals. Table III shows the average accuracy, precision, recall, and f-measure for the classes, and CNN has the highest average values for all evaluation parameters.

TABLE II

ACCURACY ANALYSIS FOR SPINALNET AND CNN ON FOUR DEMENTIA CLASSES

Methods	Accuracy of the different classes of Alzheimer's disease			
	Mild Dementia	Moderate Dementia	Non-Dementia	Very Mild Dementia
Spinal Net	86.9	87.3	87.4	88.2
CNN	96.6	97.2	97.4	98.1

TABLE III

EVALUATION OF SPINALNET AND CNN ON FOUR DEMENTIA CLASSES

Methods	Evaluation matrix			
	Avg. Accuracy	Avg. Precision	Avg. Recall	Avg. F-measure
SpinalNet	87.5	86.4	86.8	97.1
CNN	97.3	97.2	98.1	97.3

TABLE IV

EVALUATION FOR CNN AND SVC

Methods	Evaluation matrix			
	Avg. Accuracy	Avg. Precision	Avg. Recall	Avg. F-measure
SVClinear	82.4	81.8	81.7	82.2
CNN	97.6	97.8	98.4	98.1

TABLE V

PERFORMANCE EVALUATION FOR ALZHEIMER GENE EXPRESSION DATA CLASSIFIERS

Classifier	Accuracy	Precision	Recall	F-measure
KNN	64.5%	63.8%	63.7%	62.6%
SVC	82.4%	81.8%	81.7%	82.2%
Xboost	77.6%	76.4%	76.2%	75.8%

D. Performance Evaluation of Classifiers for Gene Expression Data

The analysis examines AD gene expression data and therefore the results are limited to the identification of genes using supervised classifiers. This study evaluates the comparative analysis between the three classifiers (SVC, KNN, and Xboost). We compared the CNN with SVC (using a linear kernel) (Table IV). The performance of CNN is better than SVC. Here, CNN has a better impact on the prediction of AD. Table V illustrates the evaluation performance for the classifiers. This evaluation was performed based on gene expression. For the KNN classifier, we used $k = 11$ as the number of neighbors and obtained higher accuracy than other K values. For $k = 11$, the accuracy, precision, recall, and f-measure are 64.5%, 63.8%, 63.7% and 62.6%, respectively.

Similarly, we optimized the SVC to evaluate the performance in AD. Here we used a linear kernel with a regularization parameter, $C = 17$. SVC gives the highest accuracy (82.4%) with precision (81.8%) than other classifiers. The accuracy and precision of the ensemble method used (Xboost) are 77.6% and 76.4% respectively.

We also measure the area under the receiver operating characteristic curve (ROC) (Figs. 6–8). The ranges of KNN, SVC, and xboost are 0.62, 0.84, and 0.71, respectively, and the KNN range is low and close to the baseline. However, the ranges of roc for svc and xboost are higher than those of KNN.

E. Outcomes of Explainable AI

These are the results measured using the recommended approach of explainable AI. We have described the results of the XAI method for better understanding and interpretation. To increase the interpretable mechanism of the classifiers, we used LIME. This explainable AI method describes the

Authorized licensed use limited to: VIT University- Chennai Campus. Downloaded on November 08,2022 at 05:47:25 UTC from IEEE Xplore. Restrictions apply.

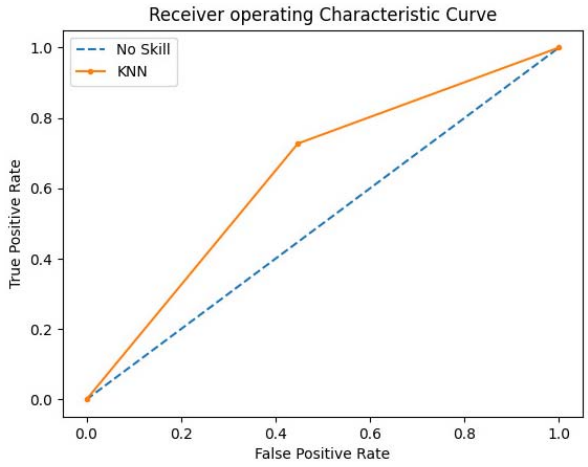

Fig. 6. Roc curve of KNN.

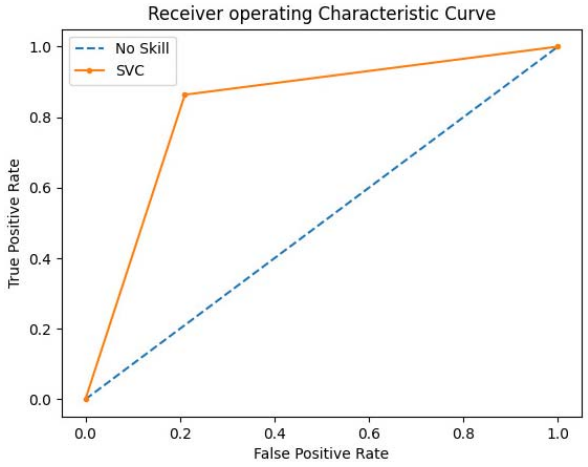

Fig. 7. Roc curve of SVC.

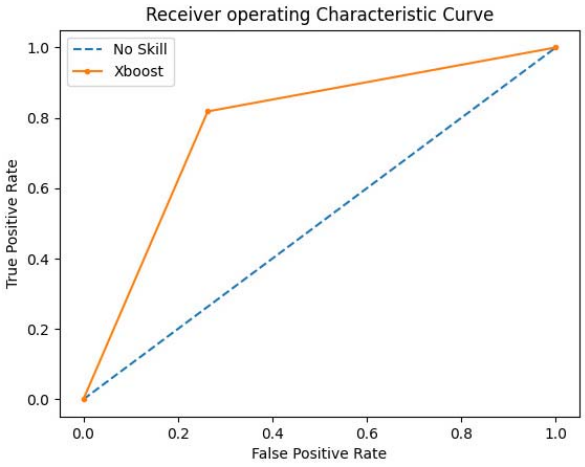

Fig. 8. Roc curve of Xboost.

role of genes. This XAI method recognized the major sets of genes for AD. We ranked the genes based on probability values. The probability values with ranked genes are shown in Fig. 9 (left), which illustrates the LIME process for AD. In Fig. 9 (left), the genes for AD and non-AD are separated and the genes are ranked based on the prediction probabilities. These probabilities were calculated using feature extraction techniques such as LASSO. LIME found the genes most

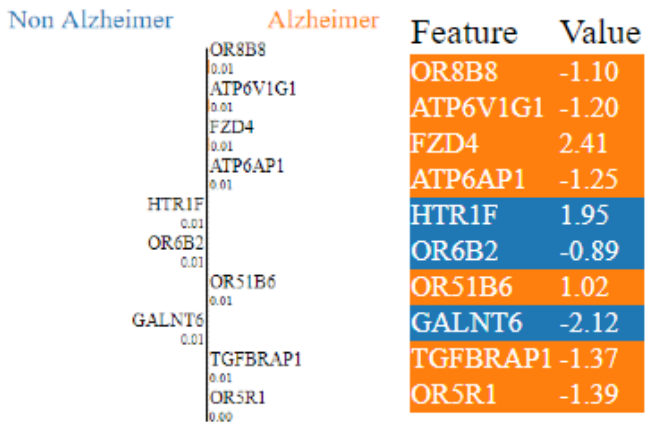

Fig. 9. LIME outcomes for SVC classifier for alzheimer patient.

responsible for AD. Fig. 9 illustrates the SVC process in which OR8B8 and ATP6V1G1 are the highly significant genes for AD and HTR1F and OR6B2 are the highly significant ones for non- AD.

IV. Conclusion

Effective and accurate diagnosis of AD is important to initiate effective treatment. In particular, early investigation of AD is expected to play an immense role in the development of cures and ultimately for the remarkable recovery of the patient. In this study, SpinalNet and CNN predict the AD classes from MRI images. CNN provides slightly better accuracy than SpinalNet in classification. We also classified the AD class from gene expression data using KNN, SVC, and Xboost classifiers. In this case, SVC is the best approach for AD classification among all applied classifiers. In this research, we have used LIME for a better understanding of the responsible AD genes. LIME explains the genes which have significance in whether one has AD or not. In the future, we can apply more interactive explainable AI, such as local interpretation-driven abstract Bayesian networks (LINDA - BN) with a DNN. We will also consider significant gene sets with the gene anomaly measures.

References

[1] A. Association, "2018 Alzheimer's disease facts and figures," *Alzheimer's Dementia*, vol. 14, no. 3, pp. 367–429, Mar. 2018.

[2] C. Trigona *et al.*, "Measurements of iron compound content in the brain using a flexible core fluxgate magnetometer at room temperature," *IEEE Trans. Instrum. Meas.*, vol. 67, no. 4, pp. 971–980, Apr. 2018.

[3] C. Trigona, V. Sinatra, B. Ando, S. Baglio, and A. Bulsara, "RTD-fluxgate magnetometers for detecting iron accumulation in the brain," *IEEE Instrum. Meas. Mag.*, vol. 23, no. 1, pp. 7–13, Feb. 2020.

[4] M. D. Hurd, P. Martorell, A. Delavande, K. J. Mullen, and K. M. Langa, "Monetary costs of dementia in the United States," *New England J. Med.*, vol. 368, no. 14, pp. 1326–1334, Apr. 2013.

[5] L. E. Hebert, J. Weuve, P. A. Scherr, and D. A. Evans, "Alzheimer disease in the United States (2010–2050) estimated using the 2010 census," *Neurology*, vol. 80, no. 19, pp. 1778–1783, 2013.

[6] C. Trigona *et al.*, "RTD-fluxgate sensor for measurements of metal compounds in neurodegenerative diseases," in *Proc. IEEE Int. Instrum. Meas. Technol. Conf. (I2MTC)*. Turin, Italy, May 2017, pp. 1–5.

[7] G. Gugliandolo *et al.*, "A movement-tremors recorder for patients of neurodegenerative diseases," *IEEE Trans. Instrum. Meas.*, vol. 68, no. 5, pp. 1451–1457, May 2019.

[8] T. G. Beach, S. E. Monsell, L. E. Phillips, and W. Kukull, "Accuracy of the clinical diagnosis of Alzheimer disease at national institute on aging Alzheimer disease centers, 2005-2010," *J. Neuropathology Experim. Neurol.*, vol. 71, no. 4, pp. 266–273, 2012.

Authorized licensed use limited to: VIT University- Chennai Campus. Downloaded on November 08,2022 at 05:47:25 UTC from IEEE Xplore. Restrictions apply.

[9] V. L. Villemagne *et al.*, "Amyloid deposition, neurodegeneration, and cognitive decline in sporadic Alzheimer's disease: A prospective cohort study," *Lancet Neurol.*, vol. 12, no. 4, pp. 357–367, 2013.

[10] K. M. Langa and D. A. Levine, "The diagnosis and management of mild cognitive impairment," *JAMA*, vol. 312, no. 23, p. 2551, 2014.

[11] C. Patterson, "World Alzheimer report 2018 the state of the art of dementia research: New frontiers," Alzheimer's Disease Int. (ADI), London, U.K., Tech. Rep., 2018. [Online]. Available: https://www.alzint.org/u/WorldAlzheimerReport2018.pdf

[12] N. S. M. Schoonenboom *et al.*, "CSF and MRI markers independently contribute to the diagnosis of Alzheimer's disease," *Neurobiol. Aging*, vol. 29, no. 5, pp. 669–675, 2008.

[13] G. B. Frisoni, N. C. Fox, C. R. Jack, P. Scheltens, and P. M. Thompson, "The clinical use of structural MRI in Alzheimer disease," *Nature Rev. Neurol.*, vol. 6, no. 2, pp. 67–77, 2010.

[14] L.-O. Wahlund, "Visual rating and volumetry of the medial temporal lobe on magnetic resonance imaging in dementia: A comparative study," *J. Neurol., Neurosurgery Psychiatry*, vol. 69, no. 5, pp. 630–635, Nov. 2000.

[15] M. Tanveer *et al.*, "Machine learning techniques for the diagnosis of Alzheimer's disease," *ACM Trans. Multimedia Comput., Commun., Appl.*, vol. 16, no. 1S, pp. 1–35, 2020.

[16] A. Heyman *et al.*, "Alzheimer's disease: Genetic aspects and associated clinical disorders," *Ann. Neurol.*, vol. 14, no. 5, pp. 507–515, 1983.

[17] D. L. Price, R. E. Tanzi, D. R. Borchelt, and S. S. Sisodia, "Alzheimer's disease: Genetic studies and transgenic models," *Annu. Rev. Genet.*, vol. 32, no. 1, pp. 461–493, Dec. 1998.

[18] R. E. Tanzi and L. Bertram, "New frontiers in Alzheimer's disease genetics," *Neuron*, vol. 32, no. 2, pp. 181–184, 2001.

[19] J. W. Ashford and J. A. Mortimer, "Non-familial Alzheimer's disease is mainly due to genetic factors," *J. Alzheimer's Disease*, vol. 4, no. 3, pp. 169–177, Jul. 2002.

[20] P. H. St George-Hyslop, "Genetic factors in the genesis of Alzheimer's disease," *Ann. New York Acad. Sci.*, vol. 924, no. 1, pp. 1–7, 2006.

[21] T. Dunckley *et al.*, "Gene expression correlates of neurofibrillary tangles in Alzheimer's disease," *Neurobiol. Aging*, vol. 27, no. 10, pp. 1359–1371, 2006.

[22] J. F. Loring, X. Wen, J. M. Lee, J. Seilhamer, and R. Somogyi, "A gene expression profile of Alzheimer's disease," *DNA cell Biol.*, vol. 20, no. 11, pp. 683–695, 2001.

[23] T. Lee and H. Lee, "Prediction of Alzheimer's disease using blood gene expression data," *Sci. Rep.*, vol. 10, no. 1, pp. 1–13, Dec. 2020.

[24] N. Xie, G. Ras, M. van Gerven, and D. Doran, "Explainable deep learning: A field guide for the uninitiated," 2020, *arXiv:2004.14545*. [Online]. Available: http://arxiv.org/abs/2004.14545

[25] S. M. Anwar, M. Majid, A. Qayyum, M. Awais, M. Alnowami, and M. K. Khan, "Medical image analysis using convolutional neural networks: A review," *J. Med. Syst.*, vol. 42, no. 11, pp. 1–13, Nov. 2018.

[26] J. Wen *et al.*, "Convolutional neural networks for classification of Alzheimer's disease: Overview and reproducible evaluation," *Med. Image Anal.*, vol. 63, Jul. 2020, Art. no. 101694.

[27] K. O'Shea and R. Nash, "An introduction to convolutional neural networks," 2015, *arXiv:1511.08458*. [Online]. Available: http://arxiv.org/abs/1511.08458

[28] H. M. D. Kabir *et al.*, "SpinalNet: Deep neural network with gradual input," 2020, *arXiv:2007.03347*. [Online]. Available: http://arxiv.org/abs/2007.03347

[29] B. Dubois *et al.*, "Research criteria for the diagnosis of Alzheimer's disease: Revising the NINCDS-ADRDA criteria," *Lancet. Neurol.*, vol. 6, no. 8, pp. 734–746, 2007.

[30] G. M. McKhann *et al.*, "The diagnosis of dementia due to Alzheimer's disease: Recommendations from the national institute on aging-Alzheimer's association workgroups on diagnostic guidelines for Alzheimer's disease," *Alzheimer's Dementia*, vol. 7, no. 3, pp. 263–269, 2011.

[31] L. Pini *et al.*, "Brain atrophy in Alzheimer's disease and aging," *Ageing Res. Rev.*, vol. 30, pp. 25–48, Sep. 2016.

[32] J. L. Whitwell *et al.*, "MRI correlates of neurofibrillary tangle pathology at autopsy: A voxel-based morphometry study," *Neurology*, vol. 71, no. 10, pp. 743–749, Sep. 2008.

[33] R. Yamashita, M. Nishio, R. K. G. Do, and K. Togashi, "Convolutional neural networks: An overview and application in radiology," *Insights Imag.*, vol. 9, pp. 611–629, Aug. 2018. [Online]. Available: https://insightsimaging.springeropen.com/articles/10.1007/s13244-018-0639-9

[34] H. Saadatfar, S. Khosravi, J. H. Joloudari, A. Mosavi, and S. Shamshirband, "A new K-nearest neighbors classifier for big data based on efficient data pruning," *Mathematics*, vol. 8, no. 2, p. 286, Feb. 2020.

[35] T. Chen and C. Guestrin, "XGBoost: A scalable tree boosting system," in *Proc. 22nd ACM SIGKDD Int. Conf. Knowl. Discovery Data Mining*. San Francisco, CA, USA: ACM, Aug. 2016, pp. 785–794.

[36] J. Cervantes, F. Garcia-Lamont, L. Rodríguez-Mazahua, and A. Lopez, "A comprehensive survey on support vector machine classification: Applications, challenges and trends," *Neurocomputing*, vol. 408, pp. 189–215, Sep. 2020.

[37] M. T. Ribeiro, S. Singh, and C. Guestrin, "'Why should i trust you?': Explaining the predictions of any classifier," 2016, *arXiv:1602.04938*. [Online]. Available: http://arxiv.org/abs/1602.04938

[38] D. S. Marcus, T. H. Wang, J. Parker, J. G. Csernansky, J. C. Morris, and R. L. Buckner, "Open access series of imaging studies (OASIS): Cross-sectional MRI data in young, middle aged, nondemented, and demented older adults," *J. Cogn. Neurosci.*, vol. 19, no. 9, pp. 1498–1507, Sep. 2007.

[39] Accessed: Aug. 3, 2021. [Online]. Available: https://central.xnat.org/

[40] S. Morabito *et al.*, "Single-nucleus chromatin accessibility and transcriptomic characterization of Alzheimer's disease," *Nature Genet.*, vol. 53, pp. 1–13, Jul. 2021.

[41] S. L. Bangare, A. Dubal, P. S. Bangare, and S. Patil, "Reviewing Otsu's method for image thresholding," *Int. J. Appl. Eng. Res.*, vol. 10, no. 9, pp. 21777–21783, 2015.

[42] S. S. Majeeth and C. N. K. Babu, "Gaussian noise removal in an image using fast guided filter and its method noise thresholding in medical healthcare application," *J. Med. Syst.*, vol. 43, no. 8, p. 280, Aug. 2019.

Authorized licensed use limited to: VIT University- Chennai Campus. Downloaded on November 08,2022 at 05:47:25 UTC from IEEE Xplore. Restrictions apply.